Metal-organic-silicon nanoscale contacts

Adam J. Dickie and Robert A. Wolkow*
Department of Physics, University of Alberta, Edmonton, Alberta, Canada T6G 2E1
and National Institute for Nanotechnology, National Research Council Canada, Edmonton, Alberta, Canada T6G 2M9
(Received 16 October 2007; published 5 March 2008)

A scanning tunneling microscope tip is used to create nanoscale contacts on degenerately doped n^+-Si(100) surfaces. Current-voltage spectra are recorded as the tip transitions from tunneling to point contact on surfaces prepared in three ways: (1) the clean 2×1 surface, (2) with a covalently bonded benzene overlayer, and (3) through nanoscale clean silicon windows formed within the benzene film. Contacts to the clean surface are more Ohmic than rectifying and show a surface leakage current that arises from partially occupied π^* states. Contacts to the benzene surface do not display a surface current and exhibit significant current rectification. The unpinning of the Si band structure by the organic adsorbate leads to inversion and a limiting minority-carrier tunnel current under reverse bias. Contacts to the windows simulate defects to an overlayer and reveal characteristics of a hybrid junction. Current-voltage spectra through the windows are free of surface leakage and are independent of the cleaned area. The return of majority carrier tunneling under reverse bias demonstrates that the pinning states of the clean substrate are restored to the windows. However, the charge distribution on the windows is significantly different from the clean surface because the restored surface states are isolated within the benzene monolayer.

DOI: 10.1103/PhysRevB.77.115305 PACS number(s): 73.63.Rt, 73.20.At, 68.37.Ef

I. INTRODUCTION

The electrical sensitivity of Si surfaces has long made them attractive materials for chemical sensors,[1] and recent work on Si nanowires demonstrates much potential.[2] The role of the metal contacts to such nanoscale devices, however, is not well understood. Scanning tunneling microscopy (STM) analysis of nanoscale metal-silicon contacts is advantageous because the junctions can be characterized both visually and electrically. Previous STM studies have shown that the reduced depletion region around nanoscale contacts increases the tunneling current density.[3,4] The narrow tunnel barriers also make the contacts quite sensitive to Si surface currents.[5,6] The surface conductance can be eliminated chemically by the adsorption of oxygen[5,7] but how this current responds to the presence of organic molecules has been unclear.

In this paper, we analyze how the conductance of a prototypical nanoscale device, an STM tip in point contact with a degenerately doped n^+-Si(100) surface, is influenced by the presence or absence of a covalently bonded benzene monolayer. Unlike clean surface contacts that reveal current-voltage (I-V) spectra due to majority carriers, the benzene-terminated surface exhibits a minority carrier current under reverse bias. Majority carrier transport is reestablished when contact is made to a nanoscale clean Si window in the benzene monolayer. Removing the π^* states of the clean surface through molecular adsorption removes a substantial surface conduction channel. Removal of surface states also unpins the Fermi level, altering the barrier associated with the space charge layer and disabling an efficient route for tunneling electrons to enter the bulk, resulting in a large—for a nanoscale contact—rectification ratio.

II. METHOD

Clean degenerately doped (As, 3 $m\Omega$ cm) n^+-Si(100)-2×1 surfaces were prepared in ultrahigh vacuum (UHV) by outgassing at 600 °C for 12 h, then annealing at 1250 °C for a few seconds. The W STM tip was cleaned in UHV by 1000 °C annealing, electron bombardment, and field emission. STM images were taken with a sample bias $V_S=-2$ V and a tunneling current $I_T=100$ pA. Current-voltage spectroscopy was performed by measuring I_T as a function of V_S ($-2-+2$ V) with the STM feedback loop switched off to ensure a constant tip position. The tip was subsequently moved 1 Å toward the surface and a new spectrum recorded. Spectra were recorded from $z'=0$ (reference position) to $z'=8$ (maximum displacement toward the surface). While recording spectra, the voltage was varied at the rate of 6 V s^{-1}. Thermal drift accounts for a 1%–2% uncertainty in the tip-sample separation. The reported spectra are the averages of 50–100 such experiments, with a relative uncertainty of 10% in the average current values. Currents were measurable from 2 pA (noise limit) to 30 nA (amplifier limit). All STM imaging and spectroscopy were performed at room temperature.

The clean n^+-Si(100)-2×1 surface was exposed to 1×10^{-6} Torr (uncorrected) of benzene vapor for 10–20 s to create a full monolayer. Local benzene desorption involved scanning the tip at $V_S=-4$ V, $I_T=400$ pA, and rates of 100–200 nm/s.[8] I-V measurements on benzene and desorbed benzene surfaces were as for the clean material, except that only a single contact was made to each desorption window. Figures 1(a) and 1(b) show STM images of the clean Si surface with ~10% defect density before and after a series of point contact experiments. The debris patterns created by contact formation have an average area of 150 nm^2.[2] The atom-scale asperities remnant on the surface after contact are imaged multiple times by several points on the somewhat blunted tip, resulting in the observed elongated images of the contact points. Figure 1(c) shows an STM image of a 400 nm^2 clean desorption window, surrounded by a benzene monolayer. The 80%–90% benzene removal rate observed in the figure was typical.

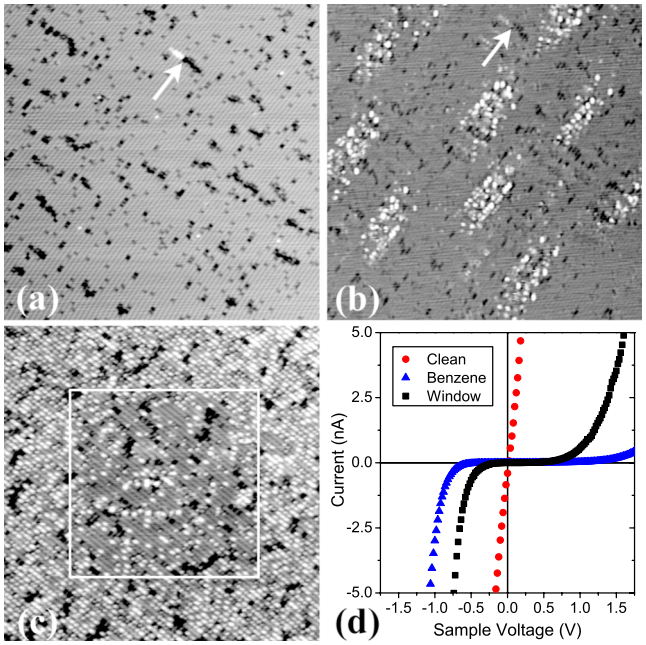

FIG. 1. (Color online) [(a) and (b)] 70×70 nm^2 UHV STM occupied state images ($V_S=-2$ V, $I_T=0.1$ nA) of n^+-Si(100)-2×1 (a) before and (b) after point contact experiments. The arrow indicates a common defect in both images. (c) STM image of a 20×20 nm^2 desorption window (outlined by white square) on benzene-covered n^+-Si(100) ($V_S=-2$ V, $I_T=0.1$ nA). (d) Linear I-V point contact ($z'=8$) characteristics on the clean, benzene-terminated, and desorption window surfaces.

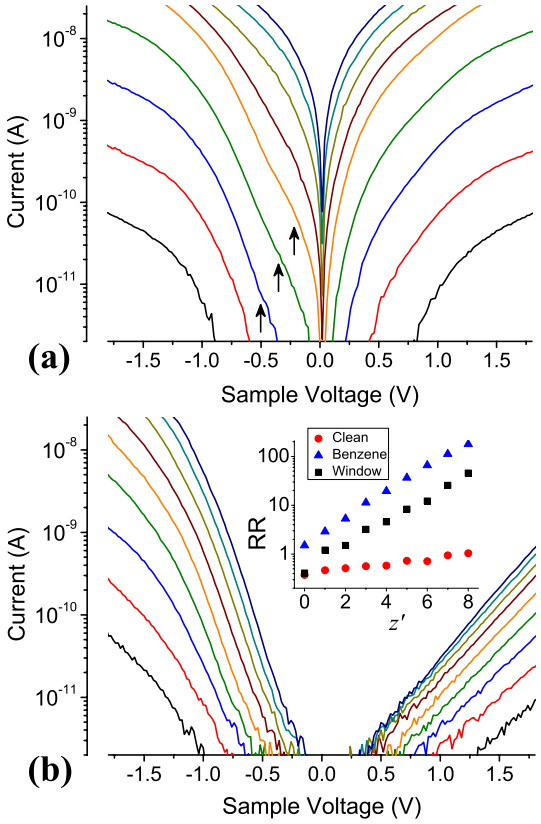

FIG. 2. (Color online) I-V spectra at tip displacements $z'=0$ (bottom curve) to $z'=8$ (uppermost curve) for (a) clean n^+-Si(100), with arrows indicating Ohmic shoulder regions; (b) benzene-terminated n^+-Si(100). Inset (b), Forward to reverse current rectification ratio (RR) at 1 V.

III. RESULTS AND DISCUSSION

A. Clean and benzene-terminated surfaces

Figure 1(d) compares the I-V spectra at point contact ($z'=8$) for contacts to clean Si, to benzene coated Si, and to clean Si within a window in a benzene overlayer. Clearly, the clean and benzene-terminated surfaces represent limiting cases of Ohmic and diode behaviors, while the window is intermediate between the two.

The effect of a molecular interface on conductance is directly seen in the semilogarithmic I-V spectra obtained during the transition from tunneling to point contact on clean and benzene-terminated n^+-Si(100) surfaces [Figs. 2(a) and 2(b)]. Contacts to the clean surface show (i) large changes in current with z' until a saturation (contact) region, (ii) nearly equal magnitudes of current under both forward (negative V_S) and reverse (positive V_S) biases, (iii) a spectrum that varies from semiconducting to Ohmic as the tip moves into contact with the surface, and (iv) an exponential increase in current with voltage until a limiting series resistance R_S dominates, i.e., $I_T\propto I_0\exp(V_S-I_TR_S)$. On the benzene surface, by contrast, the current change with z' is much smaller than on the clean substrate and shows a strong polarity dependence. The reverse spectrum is unlike the forward; it changes by a less than exponential amount with each z' increment, resulting in a 200:1 rectification ratio at point contact [inset, Fig. 2(b)]. The near linear dependence of $\ln(I_T)$ on V_S in both polarities indicates that R_S is reduced with benzene present. A finite conductance gap occurs in the spectra from tunneling to point contact.

The change in I-V spectra with tip-sample separation provides crucial insight into the mechanism of adsorbate-induced current rectification. Because the Si samples are degenerately doped, transport occurs exclusively by tunneling. Therefore, at vacuum separations, the term $d[\ln(I_T)]/dz$ measures the apparent vacuum tunnel barrier Φ_A faced by charge carriers, according to[9]

$$\Phi_A=(-(1/A)\{d[\ln(I_T)]/dz\})^2, \tag{1}$$

where $A=1.025$ eV Å^{-1} and the true separation $z=z'-z'_{contact}$. The apparent barrier is related to the ideal vacuum barrier $\Phi=[(\phi_W+\phi_{Si})/2-qV_S/2]$, where ϕ_W and ϕ_{Si} are the tip and semiconductor work functions. Φ is reduced at small tip-sample separations by interactions between the two surfaces.[10] At point contact, the vacuum barrier collapses and tunneling occurs through the depletion region formed at the metal-semiconductor interface. The transition region between contact and tunneling is indicated by a maximum in the forward bias $d^2[\ln(I_T)]/dz^2$ term, yielding contact points of $z'=5$ on the clean substrate and $z'=4$ with benzene present. In Fig. 3(a), $d[\ln(I_T)]/dz$ is plotted as a function of z for currents measured at ±1.5 V.[11] As well, tunnel current onset voltages as a function of z are shown in Fig. 3(b),

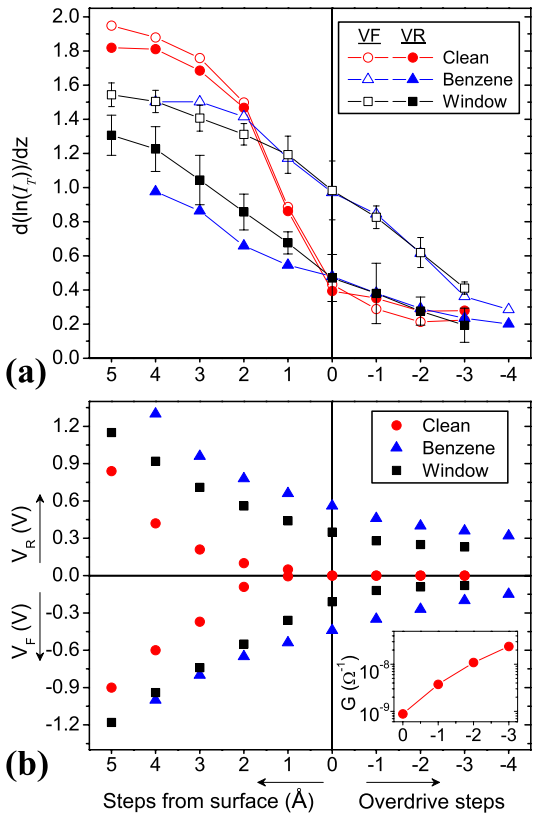

FIG. 3. (Color online) (a) Differential change in $\ln(I_T)$ with z for currents at ± 1.5 V. Window error bars are for the four spectra shown in Fig. 6 (b) 2 pA tunnel current onset voltages versus z. Inset: Zero-bias conductance versus tip overdrive for the clean surface.

providing an empirical measure of the barriers faced in vacuum and at contact.

The Si surface controls the tunneling current through the accessibility of surface states, and by the microscopic surface structure that determines ϕ_{Si}. In Fig. 4, we present a schematic model of the transport processes occurring at tunneling and point contact. Beginning with the clean (100) surface, which in the 2×1 reconstruction has bands of π and π^* states located 0.2 and 0.4 eV below the valence band (VB) and conduction band (CB) edges [Fig. 4(a)].[12] The n^+ dopant density makes the Si Fermi level (E_F) approximately degenerate with the bulk CB position at 300 K, sufficient to partially populate the acceptor π^* states and create a band bending ϕ_{Bn} of $\sim$0.7 eV.[13] The π^* states are critically important as they pin the barrier height, provide an unoccupied density of states for tunnel electrons, and create a measurable surface conductance channel that dominates the I-V spectra at short range. Si dimers on the clean 2×1 surface are buckled and have an associated surface dipole character, with the up atom negative and the down atom positive, which produces a high Si work function.

The tunnel barrier on the clean surface [Fig. 3(a)] shows little polarity dependence, suggesting a common controlling barrier in both directions. At tunnel distances, the primary component of forward current is from the VB, and in the reverse direction, electrons tunnel into the Si CB. Moving the tip toward the surface increases the tunnel penetration. In reverse bias, the onset voltage falls by half with each 1 Å increment, consistent with the behavior of electrons tunneling into a fixed barrier. In forward bias, the onset voltage drops linearly with distance as CB and surface states increasingly contribute to the tunneling. We note especially the appearance of an Ohmic shoulder in the forward current at low

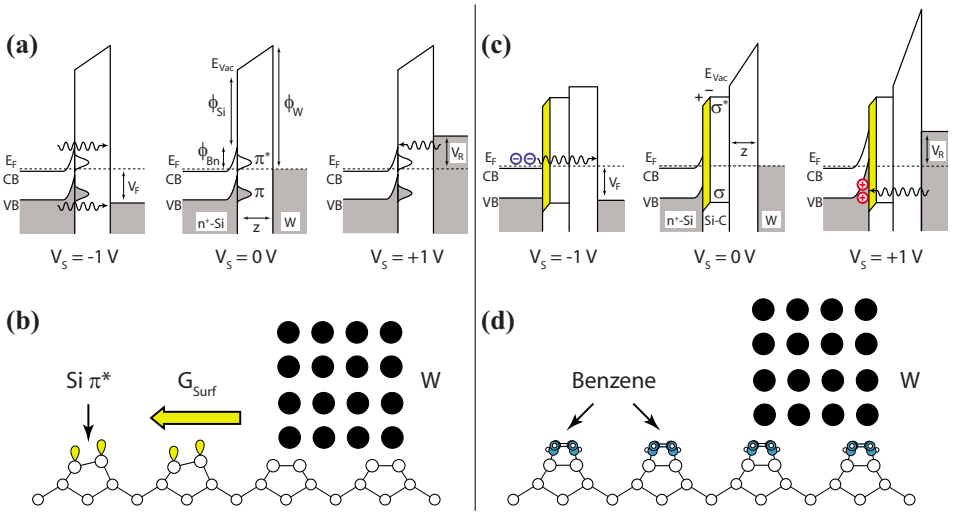

FIG. 4. (Color online) (a) Energy band diagrams for the clean surface at tunneling distance. Majority carriers tunnel under both bias polarities because the π^* states pin the barrier height and supply an unoccupied state density. (b) Model of contact geometry between the clean Si surface (open circles) and the W tip (filled circles). Bonding to the surface removes the Si dimer asymmetry, but surrounding buckled dimers with π^* states provide an Ohmic surface conductance. (c) Energy band diagrams for the benzene-terminated surface at tunneling distance. The molecular adsorption replaces the clean surface states with a dipole layer and σ/σ^* states. In forward bias, tunneling occurs only when the bands have flattened and an accumulation layer ($\ominus$) forms. In reverse bias, tunneling occurs only when the band bending is sufficient to generate a minority-carrier inversion layer ($\oplus$) in the Si, thereby rectifying the current.(d) Model of contact geometry between the benzene surface and the W tip. The monolayer fixes the Si dimer geometry and provides a finite tunnel barrier at point contact.

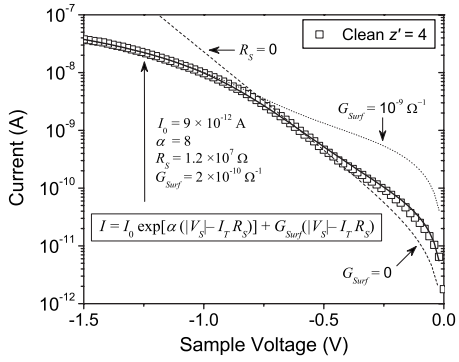

FIG. 5. Forward bias *I-V* spectrum at 1 Å ($z'=4$) above the clean surface (symbols) and theoretical fits (lines) obtained with Eq. (2). The solid line shows the best fit with parameters listed in the legend. An identical fit, but with an order of magnitude increase in G_{surf}, is given by the dotted line. Similarly, the dashed line demonstrates the theoretical fit with the surface conductance and series resistance turned off.

biases (0 to −0.5 V) and small tip-sample separations [$z'=2-4$ in Fig. 2(a)]. This is a familiar indication of a leakage current through a diode,[14] which we attribute to a parallel surface state conduction channel only observable at close separations because of the small decay length of these states. An empirical fit to the equation

$$I_T = I_0 \exp[\alpha(|V_S| - I_T R_S)] + G_{surf}(|V_S| - I_T R_S), \qquad (2)$$

where I_0 and α are adjustable parameters [corresponding to the intercept at $V_S=0$ and the slope of $\ln(I_T)/V_S$, respectively] and R_S is extracted from the slope of I_T/V_S at $V_S \geqslant -1.5$ V, yields $G_{surf}=10^{-12}-10^{-10}\ \Omega^{-1}$ for $z'=2-4$ in Fig. 2(a). The surface conductance is clearest at 1 Å from the surface, and in Fig. 5, we show this *I-V* spectrum along with theoretical fits obtained using Eq. (2). At point contact, the conductance gap disappears and a zero-bias conductance of $10^{-9}-10^{-8}\ \Omega^{-1}$ is observed with overdrive into the Si [inset, Fig. 3(b)]. We note that a lower-doped (1 Ω cm) clean n^+-Si(100)-2×1 sample yields a much decreased zero-bias conductance at contact, on the order of $10^{-11}\ \Omega^{-1}$. These dopant concentration dependent results show that the magnitude of surface conductance is related to the partial electron population of the π^* states.

When metal touches the clean Si surface and undergoes atom to atom bonding, then the buckle asymmetry of 2×1 dimers and associated π^* pinning centers will disappear [Fig. 4(b)]. The change in surface structure with contact is reflected by the sharp decrease in $d[\ln(I_T)]/dz$ from 2 Å above the interface [Fig. 3(a)]. However, immediately adjacent to those contact points are surviving Si dimers and therefore pinning still applies, as evidenced by the Ohmic *I-V* spectra in this region [Fig. 1(d)].

Benzene adsorbs on the Si(100)-2×1 surface via a [2+2] cycloaddition to replace the Si dimer π and π^* surface states with σ states that cannot serve to localize charge at the surface [Fig. 4(c)].[15] The elimination of surface charge flattens and unpins the bands, which has two effects on the *I-V* spectra. First, in the presence of the STM tip, a distance-dependent Schottky barrier is formed with an approximate value of $\phi_{Bn}=\phi_W-\phi_{Si}$ at point contact. Second, with the Si bands following the applied voltage and an insulating molecular layer on the surface, the tunneling contacts to the benzene-terminated samples behave as metal-insulator-semiconductor (MIS) diodes.

In forward bias on the benzene surface, tunneling occurs only when the potential is sufficient to bend the Si bands down, flattening the Schottky barrier and creating an accumulation region at the surface. Forward current in the clean surface contact is fundamentally different; there, tunneling readily occurs, even at small applied bias, through the pinned depletion region to surface states. A large difference in tunnel onset voltages therefore results [Fig. 3(b)]. Tunnel barriers also decrease markedly from clean values [Fig. 3(a)] which reflects the change in surface structure. Adsorbing benzene symmetrizes the Si surface dimers and creates a weakly polarized Si-C bond, with the net effect being a lower ϕ_{Si} (less negatively charged interface) than the clean surface.

The organic interface has the effect of greatly inhibiting reverse tunneling as follows. Increasing reverse voltage does little to improve injection into the conduction band because the surface bands follow the tip potential. Current onset results when bias is sufficient to bend the VB close to the Fermi level, creating an inversion layer of holes at the surface, which tip-derived electrons can tunnel to [Fig. 4(b)]. This minority-carrier controlled current is limited by the hole generation rate and the hole diffusion radius within the semiconductor, not by the tunneling distance.

With contact to the benzene surface [Fig. 4(c)], an abrupt change in surface structure does not occur, as evidenced by the slow decay of the forward $d[\ln(I_T)]/dz$ term [Fig. 3(a)]. The monolayer constrains the Si dimers to the symmetric position and acts as an intermediate layer between the tip and Si. A flatband voltage of −0.4 V and an inversion voltage of +0.6 V is required for tunnel currents at point contact, in approximate agreement with the Si band gap. No surface conductance is observed with the monolayer present. With overdrive into the surface, it is certain that the benzene layer is breached and direct metal-Si bonds form. This is evident in the decreasing conductance gap with tip overdrive, but, crucially, the character of the clean Si contact does not return, indicating a dominant effect of the chemically terminated surrounding surface on the contact conductance.

Further evidence for MIS behavior of the benzene surface comes from the reduced series resistance revealed in the *I-V* spectra. The major component of R_S for point contacts is a spreading resistance[16] where the current is limited by the diffusive carrier transport to the surface. On the clean sample, R_S is relatively high because the surface is pinned, creating an unchanging barrier and a voltage drop through the Si surface depletion region. On the benzene surface, the bands flatten under forward bias, causing a decrease in R_S. Under reverse bias, the benzene surface current is limited by diffusion of holes generated within a diffusion length of the contact, and R_S is minimized.

B. Clean windows on the benzene surface

Figure 6 shows semilogarithmic *I-V* spectra for several clean silicon windows created within the benzene monolayer.

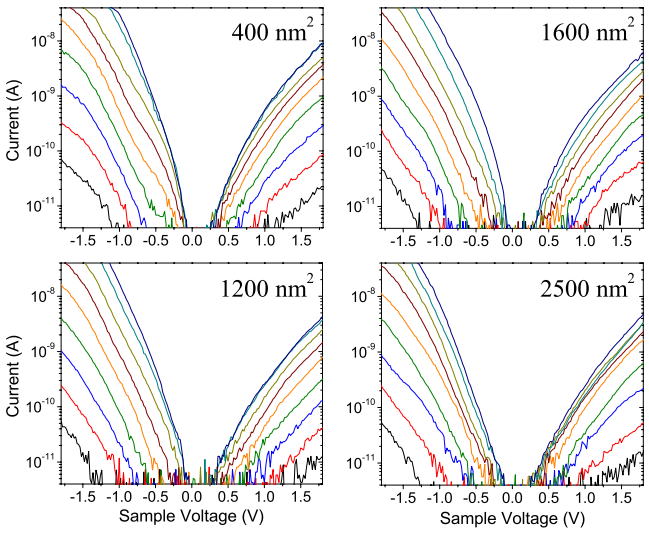

FIG. 6. (Color online) Single-measurement *I-V* spectra at tip displacements $z'=0$ (bottom curve) to $z'=8$ (uppermost curve) for desorption windows with areas of 400–2500 nm^2 on the benzene-terminated n^+-Si(100) surface.

The window contacts are hybrids, displaying attributes of the clean and the benzene-covered surfaces. We observe little dependence of the window conductance properties on desorption area, with cleaned areas from 400 to 2500 nm^2 producing nearly identical spectra.

Reverse current through the window contacts reveals an exponential dependence on distance [Fig. 3(a)], indicating a return to majority carrier tunneling upon restoration of Si π^* states and pinning. Pinning is evident in the return of R_S-induced curvature in the semi-logarithmic *I-V* spectra. Previous work has demonstrated that it is possible to change an MIS tunnel diode into a majority (barrier limited) or minority (generation limited) device by using metals with different work functions to alter Schottky barrier heights.[17] Here, we show a fundamentally different mechanism that leads to a similar carrier switching effect.

A decrease in the onset voltage observed for the windows relative to the benzene surface [Fig. 3(b)] occurs because of tunneling contributions from the Si surface states. However, the absence of a strong zero-bias conductance and the striking independence of spectra on desorption area allows us to conclude that π^* states are required across the surface, not only near the contact, to reestablish the substantial clean surface conductance channel. We might surmise that the window *I-V* spectra represent the true character of a nanoscale metal-semiconductor contact—free of extraneous effects. That proposal was not supported by a simple test. Subtracting the calculated G_{surf} term [Eq. (2)] from the clean Si *I-V* spectra produces onset voltages identical to the window values, but current magnitudes measured for the window contacts were far less than for the corrected clean surface spectra.

One further important characteristic of the window contacts is that the change in forward $d[\ln(I_T)]/dz$ is identical to the data recorded over the benzene surface, implying a similar surface work function. In turn, this result indicates that the surface charge on the window Si dimers is less negative than that on the pristine 2×1 surface. The evident electronic differences between the clean and window surfaces occur because the band bent window regions are adjacent to the relatively low energy conduction band edge of the benzene-terminated region. Lateral interactions depopulate the Si π^* states somewhat and lessen window band bending, in accordance with the empirical observation that R_S (clean) $>R_S$ (window). We expect that window dimensions on the order of the minority carrier diffusion length (~1 μm) would be required to reproduce the original clean surface charge.

IV. SUMMARY

Summarizing, the clean surface contacts appear more Ohmic than rectifying. This is expected because the narrow space charge barrier associated with nanoscale contacts allows a substantial reverse bias leakage. Furthermore, the surface leakage channel, whether due to π^* band conductance or a space charge established by pinning by the π^* states, is in any case expected to be Ohmic in character. Contacts to the benzene surface show no surface leakage channel and exhibit a significant current rectification. The essential character of the benzene contact is related to the removal of pinning, leading to flatbands and low R_S. Under reverse bias, unpinning leads to inversion and minority-carrier dominated current.

The window contacts, much like defects in a monolayer, reveal characteristics of both the organic film and the clean semiconductor. The window contacts show the pinned character of the clean surface, including the majority carrier reverse current. Despite the seeming capacity of the partially occupied surface π^* band within the window to link metal states to bulk silicon states, the window contacts do not exhibit a large contact area character. Indeed, the window contacts conduct more poorly than the clean surface contacts with surface conduction contributions removed. Because the restored Si π^* states are surrounded by the benzene monolayer, charge in the window region is somewhat diminished compared to the clean surface resulting in altered contact properties.

It is certain that nanoscale surface contacts will be of variable character if surface cleanliness is variable. It is evident that adsorption events near uncontrolled contacts to a semiconductor, including nanowire sensors, might be mistaken as conductance changes thought due to adsorbate-induced channel resistance modulation in field effect devices.

ACKNOWLEDGMENTS

We gratefully acknowledge Moh'd Rezeq and Joachim Burghartz who initiated the experiments on STM point contacts. We thank Jason Pitters for valuable technical advice. This work was supported by the National Research Council of Canada, the University of Alberta, NSERC, CIAR, and iCORE.

*rwolkow@ualberta.ca

[1] W. H. Brattain and J. Bardeen, Bell Syst. Tech. J. **32**, 1 (1953).
[2] E. Stern, J. F. Klemic, D. A. Routenberg, P. N. Wyrembak, D. B. Turner-Evans, A. D. Hamilton, D. A. LaVan, T. M. Fahmy, and M. A. Reed, Nature (London) **445**, 519 (2007).
[3] G. D. J. Smit, S. Rogge, and T. M. Klapwijk, Appl. Phys. Lett. **80**, 2568 (2002).
[4] O. Kubo, Y. Shingaya, M. Aono, and T. Nakayama, Appl. Phys. Lett. **88**, 233117 (2006).
[5] P. Avouris, I.-W. Lyo, and Y. Hasegawa, J. Vac. Sci. Technol. A **11**, 1725 (1993).
[6] R. Hasunuma, T. Komeda, and H. Tokumoto, Appl. Surf. Sci. **130-132**, 84 (1998).
[7] C. Petersen, F. Grey, and M. Aono, Surf. Sci. **377-379**, 676 (1997).
[8] P. Kruse and R. A. Wolkow, Appl. Phys. Lett. **81**, 4422 (2002).
[9] N. D. Lang, Phys. Rev. B **37**, 10395 (1988).
[10] M. Weimer, J. Kramar, and J. D. Baldeschwieler, Phys. Rev. B **39**, 5572 (1989).
[11] An empirical fit given by Eq. (2) was used to approximate I_T at ± 1.5 V for currents truncated by the amplifier limit.
[12] F. J. Himpsel and T. Fauster, J. Vac. Sci. Technol. A **2**, 815 (1984).
[13] P. Mårtensson, A. Cricenti, and G. V. Hansson, Phys. Rev. B **33**, 8855 (1986).
[14] J. H. Werner, Appl. Phys. A: Solids Surf. **47**, 291 (1988).
[15] G. P. Lopinski, T. M. Fortier, D. J. Moffatt, and R. A. Wolkow, J. Vac. Sci. Technol. A **16**, 1037 (1998).
[16] F. Flores and N. Garcia, Phys. Rev. B **30**, 2289 (1984).
[17] M. A. Green, F. D. King, and J. Shewchun, Solid-State Electron. **17**, 551 (1974).